Theor Chem Acc (2001) 105:207–212
DOI 10.1007/s002140000203

Theoretical
Chemistry Accounts

Regular article

Transition structure selectivity in enzyme catalysis: a QM/MM study of chorismate mutase

Sergio Martí[1], Juan Andrés[1], Vicent Moliner[1], Estanislao Silla[2], Iñaki Tuñón[2], Juan Bertrán[3]

[1] Departament de Ciències Experimentals, Universitat Jaume I, Box 224, 12080 Castellón, Spain
e-mail: moliner@exp.uji.es, Fax: +34-964-728066
[2] Departament de Química Física, Universidad de Valencia, 46100 Burjasot, Valencia, Spain
e-mail: ignacio.tunon@uv.es, Fax: +34-963-864564
[3] Departament de Química, Universidad Autónoma de Barcelona, 08193 Bellaterra, Barcelona, Spain

Received: 25 March 2000 / Accepted: 7 August 2000 / Published online: 23 November 2000

Abstract. Two different transition structures (TSs) have been located and characterized for the chorismate conversion to prephenate in *Bacillus subtilis* chorismate mutase by means of hybrid quantum-mechanical/molecular-mechanical (QM/MM) calculations. GRACE software, combined with an AM1/CHARMM24/TIP3P potential, has been used involving full gradient relaxation of the position of ca. 3300 atoms. These TSs have been connected with their respective reactants and products by the intrinsic reaction coordinate (IRC) procedure carried out in the presence of the protein environment, thus obtaining for the first time a realistic enzymatic reaction path for this reaction. Similar QM/MM computational schemes have been applied to study the chemical reaction solvated by ca. 500 water molecules. Comparison of these results together with gas phase calculations has allowed understanding of the catalytic efficiency of the protein. The enzyme stabilizes one of the TSs (TS_{OHout}) by means of specific hydrogen bond interactions, while the other TS (TS_{OHin}) is the preferred one in vacuum and in water. The enzyme TS is effectively more polarized but less dissociative than the corresponding solvent and gas phase TSs. Electrostatic stabilization and an intramolecular charge-transfer process can explain this enzymatically induced change. Our theoretical results provide new information on an important enzymatic transformation and the key factors responsible for efficient selectivity are clarified.

Key words: Chorismate mutase – Rearrangement – Enzyme catalysis – Ab initio calculations – Quantum mechanics-molecular mechanics

1 Introduction

The rearrangement of chorismate to prephenate is a Claisen reaction catalyzed by the enzyme chorismate mutase [1, 2]. This reaction proceeds through a chair-like transition state with a concerted but asynchronous break of a carbon-oxygen bond and formation of a new carbon-carbon bond (see Scheme 1) [3, 4] and is one of the few examples of enzyme-catalyzed pericyclic reactions [5].

Understanding the catalytic action depends on the knowledge of geometrical and electronic properties of the transition structure (TS) in the enzyme active site [6]. Many different theoretical studies have been devoted to the study of this rearrangement in the gas phase or in aqueous solution [7–10] and in models of real enzymatic environments [11–13]. A recent study [7] combining gas phase theoretical calculations and kinetic isotopic effects measured for the *Bacillus subtilis* chorismate mutase enzyme (BsCM) arrived at the conclusion of a very dissociative and highly polarized TS in the enzyme.

The results we present in this paper are, to our knowledge, the first time that the TS is properly located and characterized and the intrinsic reaction coordinate path (IRC) procedure traced down to the reactants and products in the enzymatic active site. For this purpose we use hybrid quantum mechanics-molecular mechanics (QM/MM) methods based on the concept introduced by Warshel and Levitt in 1976 [14]. Previous studies using this methodology were restricted to partial geometry optimizations following gas phase reaction paths or approximated strategies (i.e. fixing the MM part of the system) [11, 12]. Our results show that the TS is largely polarized by the enzymatic environment but is less dissociative than expected as far as the enzyme induces a shortening of the bond breaking and bond forming distances with respect to the gas phase and solution results.

The chorismate to prephenate rearrangement is preceded by an equilibrium between diequatorial and diaxial forms of chorismate (see Scheme 2). The diequatorial arrangement is the most populated structure in the gas phase but the diaxial arrangement is the reactive conformer capable of progressing to the TS. As we show, there exist at least two diaxial structures relevant for this

Correspondence to: V. Moliner and I. Tuñón

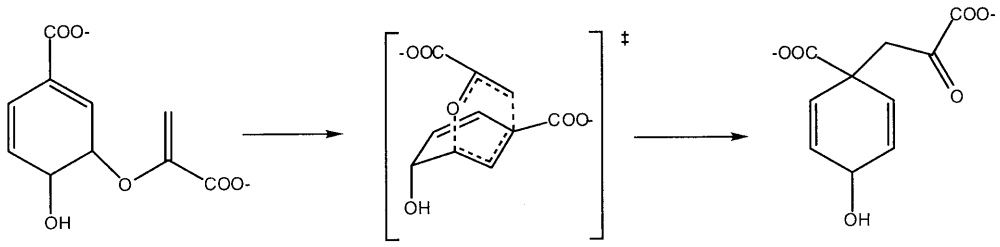

Scheme 1 Rearrangement of chorismate to prephenate

process, each one giving place to a different reaction path leading to prephenate through two different TSs, which mainly differ in the orientation of the hydroxyl group with respect to the ring (TS_{OHin} and TS_{OHout}). The change in the OH orientation has also noticeable consequences on bond breaking C-O and bond forming C-C processes. In this paper we try to systematize the results in terms of two different reaction paths, showing that the enzyme selectively stabilizes one of them.

2 Computational methods

Calculations in the gas phase have been carried out at the AM1 [15] and B3LYP/6-31G* levels [16] using the GAUSSIAN94 package of programs [17]. Minima and transition structures have been located using the Berny's algorithm [18] and they have been characterized by inspection of the analytical Hessian matrix, which has one and only one negative eigenvalue in the case of the TS.

QM/MM calculations in solution have been carried out using CHARMM24b2 [19] and GRACE [20] programs. The reacting system was treated by the AM1 semiempirical molecular orbital method, placed in a cavity deleted from a 15 Å radius sphere of 488 water molecules described by the TIP3P empirical potentials. A solvent boundary potential was employed to prevent evaporation of water molecules from the surface of the resulting sphere.

For the QM/MM enzyme calculations we also employed the CHARMM24b2 and GRACE programs. The structure of the chorismate mutase enzyme has been obtained from *Bacillus subtilis* in the Protein Data Bank (PDB) [21]. CHARMM24 was used to add hydrogens to all titratable residues at a state complementary to pH 7. The system was placed in a cavity deleted from a preequilibrated 15 Å radius sphere of TIP3P water molecules centered on the substrate. The full system was divided into a QM region of 24 atoms, the substrate molecule, treated by the AM1 semiempirical MO methods, and a MM region, comprising the enzyme trimer plus crystallization and solvation water molecules (5573 enzyme atoms plus 224 non-rigid TIP3P water molecules). During the enzyme optimizations the QM atoms and the MM atoms lying in a sphere of 18 Å of radius centered on the QM system were allowed to move (a total of 3349 atoms).

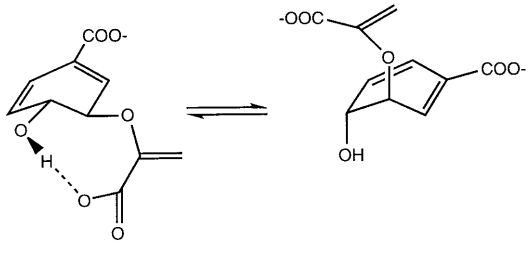

Scheme 2 Diequatorial and diaxial conformational equilibrium of chorismate reactants

QM/MM stationary points location and characterization were guided by means of the GRACE program, which use a Newton-Raphson algorithm with a Hessian matrix of 72×72 order, describing the curvature of the QM/MM energy hypersurface for a sub-set of the system (the QM part), together with a diagonal Hessian plus updates for the rest of the system. Finally, the IRC path was traced down to reactants and products valleys. As described in a previous paper [20b], the IRC calculations employed a modified version of the MOPAC routine based on the method of Gordon and co-workers [22]. The initial step was done in the direction of the transition vector from diagonalization of the mass-weighted explicit Hessian. Subsequent steps along the IRC utilized the gradient vector for the QM atoms computed with full relaxation of the MM atoms; the difference between this and the true IRC using the full gradient vector is trivial since the contribution from atoms outside the core is negligible. It was essential to use a small step size in the IRC computation in order to allow the environment to relax at every single step and then to prevent the algorithm halting falsely.

3 Results and discussion

Figure 1 shows the stationary structures found along the two reaction paths (OHin and OHout) obtained in the gas phase, while the energy profiles calculated at the three different environments are shown in Fig. 2. Selected geometrical parameters, charge transfer and energetic values for both pathways are presented in Table 1. An analysis and comparison of the gas phase reported results show that AM1 and B3LYP/6-31G* descriptions of the reaction paths are in qualitative good agreement. Nevertheless, some differences can be found, such as the larger values of the activation barriers at the AM1 level than at the B3LYP one. The diaxial chorismate conformer corresponding to the OHout path is considerably more stable than the OHin diaxial chorismate (6.3 kcal/mol and 14.9 kcal/mol at the AM1 and B3LYP/6-31G* levels, respectively). This fact can be explained because in the former there is an intramolecular hydrogen bond between the hydroxyl

group of the ring and an oxygen atom of the closer carboxylate group. This hydrogen bond disappears at the TS (both TS_{OHout} and TS_{OHin}). A favorable interaction between the hydroxyl hydrogen atom and the π-electrons of the ring system is presented in the TS_{OHin} structure. Therefore, TS_{OHin} has now a lower energy than TS_{OHout} (2.4 and 3.0 kcal/mol at the AM1 and B3LYP/6-31G* levels, respectively).

An analysis of the geometrical parameters at both TSs shows that the bond breaking (C-O) distance presents shorter values than the bond forming (C-C) distance. Larger values for both distances are calculated at the B3LYP/6-31G* level than at the AM1 one. The bond breaking process (C-O distance of 1.854/2.275 Å at the AM1/B3LYP levels, respectively) is more advanced at the TS_{OHout} than at the TS_{OHin} (C-O distance of 1.824/2.100 Å at the AM1/B3LYP levels, respectively). The opposite result is found for the bond forming process: at TS_{OHout} the values of the C-C distances are 2.164/2.719 at the AM1/B3LYP levels, respectively, while at TS_{OHin} these values are 2.120/2.573. Therefore, in the gas phase, TS_{OHout} is somewhat more dissociative than the TS_{OHin}.

Environment effects are expected to have a dramatic influence on these two competitive reaction paths. For instance, the hydroxyl hydrogen orientation can be highly determined by specific interactions with surrounding molecules or groups in the active site of the enzyme, as well as with water molecules of the solvated system. In this sense, previous theoretical studies using a continuum model of aqueous solution show a diminution of the energy gap between both TSs [8]. Monte Carlo studies with discrete solvent molecules have been carried out only for TS_{OHout} [7, 8], while previous calculations in enzymatic environment always used the OHin reaction path [11, 12], because it is the one with a lower barrier in the gas phase. In one of these works [11] the OH group was rotated to maximize its interactions with the environment.

In this paper we localize and characterize both TSs in the presence of discrete water molecules and in the active site of BsCM. We have also traced down the reaction paths towards the corresponding reactants and products. Both reaction profiles obtained by means of QM/MM calculations are shown in Fig. 2. It can be easily seen at first glance that the enzyme selectively stabilizes the OHout reaction path. The energy difference between both TSs is now 7.7 kcal/mol, TS_{OHout} being the the most stable. This means that TS_{OHout} is stabilized in the enzyme 10.1 kcal/mol more than TS_{OHin}. As shown before, the AM1 method reproduces quite well the energy differences between both TSs in the gas phase, and thus this result can be taken as being quite reliable. The TS favored in solution is, as for the gas phase calculations, the OHin, although now the energy difference between both TSs is only 0.44 kcal/mol.

Based on the analysis of the hydrogen bond interactions of the substrate with the closest residues, the origin of the enzyme selectivity can be analyzed. Both TSs located in solution and in the enzyme active site are depicted in Figs. 3 and 4. The hydrogen bonding pattern of the two transition structures is quite similar except with respect to the hydroxyl group. From the solvated system point of view, the hydrogen bonds with the water

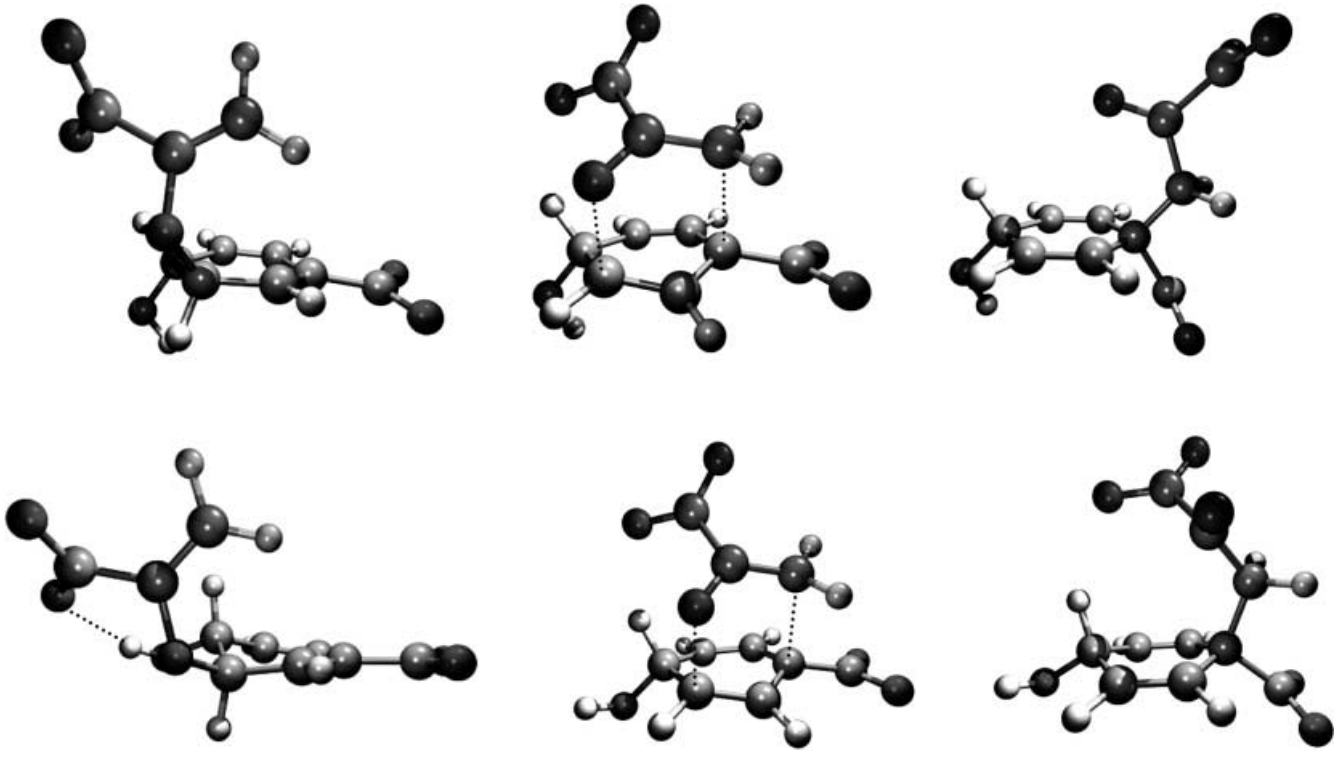

Fig. 1. Gas phase stationary structures (reactants, transition structure, and products) for the OHin (*top*) and OHout (*bottom*) reaction paths

molecules are slightly favored in the case of the OHout conformer if compared with the OHin one. We can rationalize this result as due to the steric hindrance of the latter. As expected, the enzyme environment is more specific. In the TS_{OHout}, the hydroxyl oxygen atom forms a hydrogen bond with Cys75, while the hydroxyl hydrogen atom interacts with the carboxylate group of Glu78. However, in the TS_{OHin}, the hydroxyl oxygen atom accepts the hydrogen atom from Cys75 but the hydroxyl hydrogen atom is now directed toward Ala59, and thus it cannot take part in a hydrogen bond. The rest of enzyme TS interactions are quite similar in both cases. The carboxylate group of the ring interacts with three water molecules and there is an additional water molecule bridging between one of these water molecules and the ether oxygen. This oxygen atom also takes part in a hydrogen bonding interaction with Arg90. These interactions between the environment and the ether oxygen are expected to lower the barrier height [8, 12]. The other carboxylate group is stabilized by means of hydrogen bonds with two arginine residues (Arg7 and Arg90), one tyrosine (Tyr108), and a water molecule. There is also a favorable interaction between the ring and the methyl group of Ala59. The structure obtained with the present model is in good agreement with X-ray data of a complex of BsCM with an inhibitor that mimics the TS of the reaction [23].

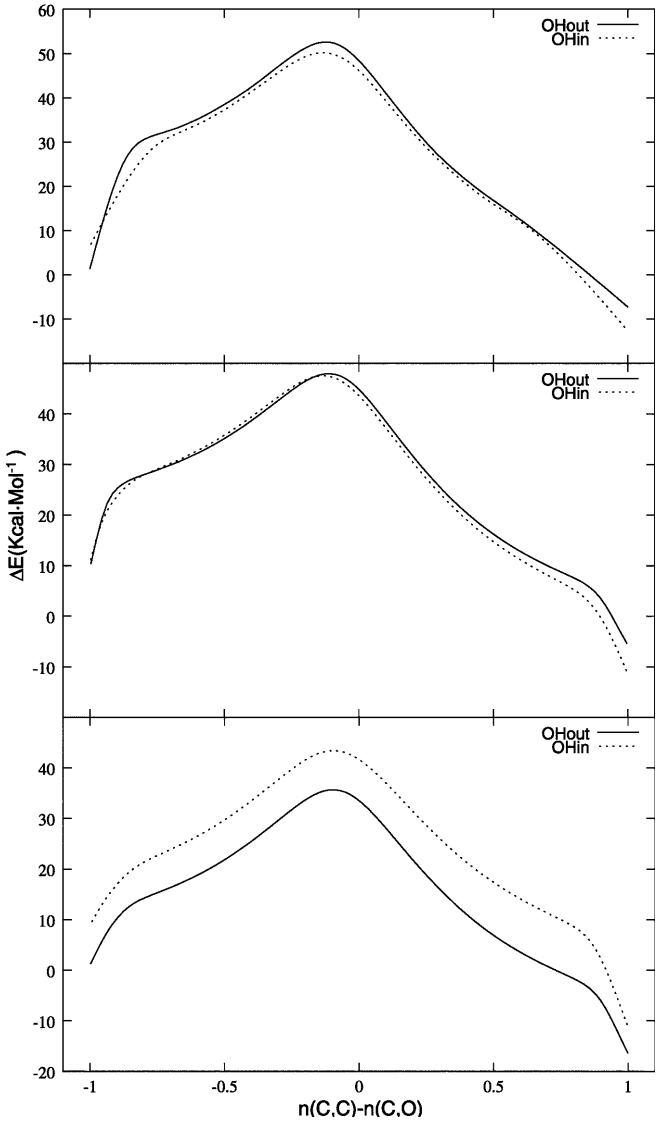

Fig. 2. Gas phase (*top*), in water (*middle*), and enzymatic (*bottom*) energy profiles for the OHin and OHout reaction paths versus the difference between the bond orders for the forming and breaking bonds

The conjunction of these interactions at the TS results in considerabe catalysis of the reaction. The energy barriers at the AM1 level are lowered from 44.01/52.74 kcal/mol in the gas phase to 47.57/44.12 kcal/mol obtained in the solvated system and 35.12/35.73 kcal/mol in the enzyme active site, for the OHin/OHout paths, respectively. This gives a rate enhancement of about 10^6–10^7, to be compared with the experimental ratio of aqueous solution and enzymatic rate constants which has been measured to be about 10^6 [24]. It is also worth noting that because of the interactions between the hydroxyl group of the substrate and the water molecules or Glu78 residue, the OHout chorismate reactant does not keep its intramolecular hydrogen bond. The same argument can be applied for the solvated system, being in this case the solute-solvent interactions responsible for this hydrogen bond breaking. The consequence of this loss of intramolecular interaction is a decrease of the relative energy of both chorismate conformers when going from gas phase calculations to the aqueous or enzymatic QM/MM ones (6.3, 3.9, and 8.3 kcal/mol, respectively).

Table 1. Distances (in Å), intramolecular charge tranfer (in a.u.), and energies (in kcal/mol) for TS_{OHin} and TS_{OHout} in the gas phase in water, and in the BsCM (AM1/CHARMM)

Method		d_{CC}	d_{CO}	ΔQ^a	$\Delta E^{\ddagger b}$	$\Delta E_{TS}{}^c$
B3LYP/6-31G*	TS_{OHin}	2.573	2.100	0.25	26.15	–
	TS_{OHout}	2.719	2.275	0.33	44.07	−3.02
AM1	TS_{OHin}	2.120	1.824	0.20	44.01	–
	TS_{OHout}	2.164	1.854	0.26	52.74	−2.40
QM/MM (water)	TS_{OHin}	2.112	1.826	0.39	47.57	–
	TS_{OHout}	2.149	1.874	0.44	44.12	−0.44
QM/MM (enzyme)	TS_{OHin}	2.063	1.833	0.38	35.12	–
	TS_{OHout}	2.116	1.869	0.46	35.73	7.72

[a] $\Delta Q = \sum_{ring} Q - \sum_{bridge} Q$ (Q being the atomic Mulliken charges)
[b] Relative energy between TS and the corresponding chorismate reactant
[c] Energy difference between TS_{OHin} and TS_{OHout}

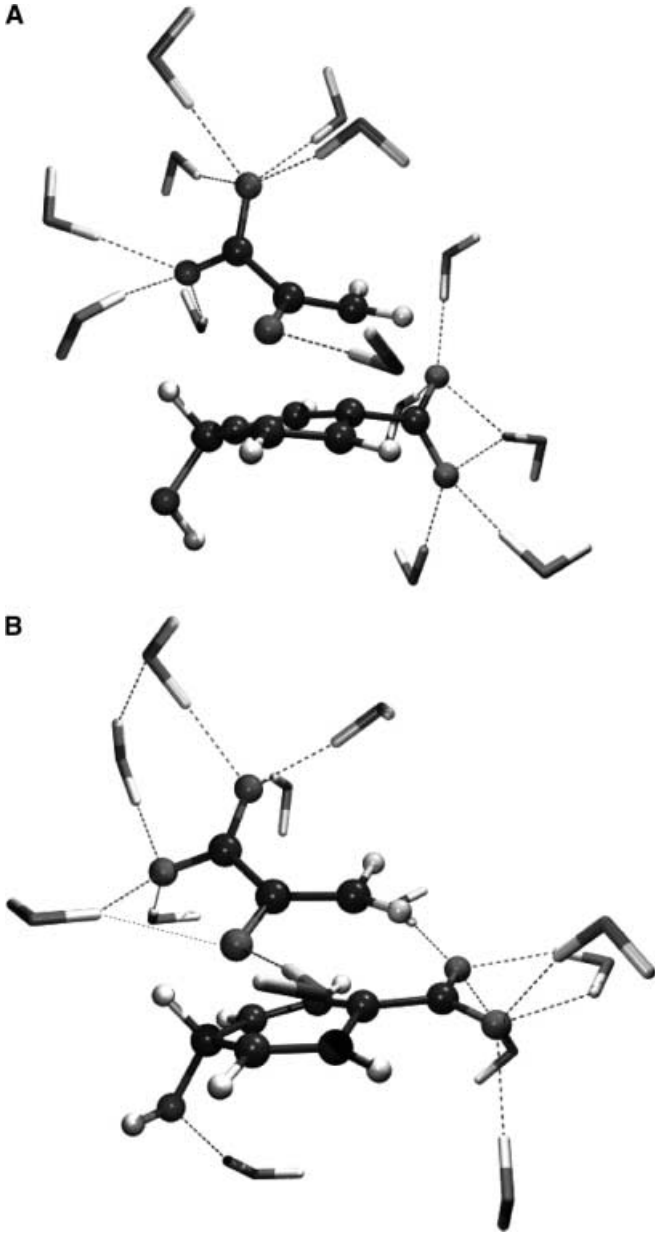

Fig. 3. OHin (*top*) and OHout (*bottom*) QM/MM transition structures in a cavity deleted from a 15 Å radius sphere of water molecules. For clarity purposes, only the hydrogen bonded water molecules are shown

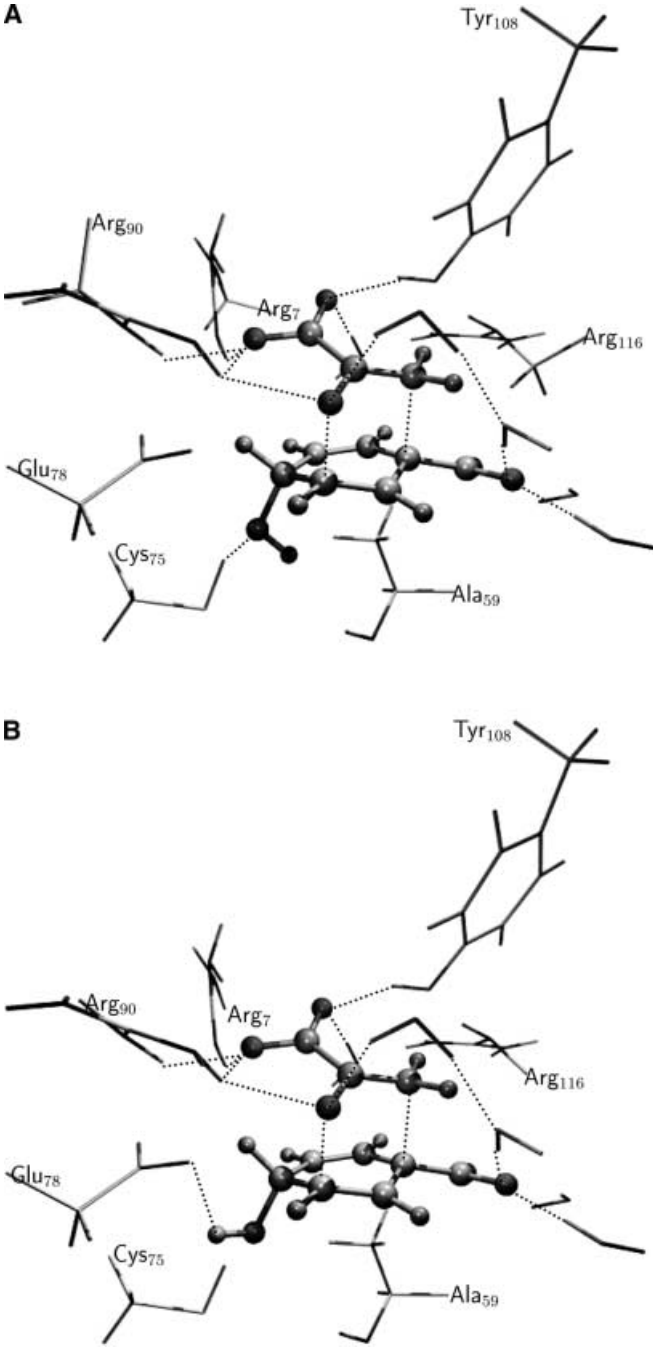

Fig. 4. OHin (*top*) and OHout (*bottom*) QM/MM transition structures in the active site of the BsCM enzyme. For clarity purposes, only the closest residues and water molecules are shown

The diminution of the OHout barrier energy obtained in water can be also interpreted by means of a deformation of the reactant towards the saddle point structure, instead of a TS stabilization.

An analysis and comparison of the geometrical results in gas phase and in the presence of solvent or enzyme environment, reported in Table 1, shows that both TSs obtained when the enzymatic effect is included are less dissociative than the gas phase structures. For the OHin reaction path the C-O and C-C bond distances are reduced/increased from 2.120 and 1.824 Å in the gas phase to 2.063 and 1.833 Å in the enzyme, respectively. For the OHout path the same distances are reduced/increased from 2.164 and 1.854 Å to 2.116 and 1.869 Å, respectively. The calculations carried out in the presence of the water sphere render results in between these figures. A measure of the asynchronicity, given by $AS = d_{CC} - d_{CO}$, shows that the enzymatic TSs are more synchronous than the gas phase ones. The AS values in the gas phase are 0.30 and 0.31 Å for TS_{OHin} and TS_{OHout}, respectively, 0.29 and 0.28 Å in the water environment, respectively, and in the enzyme they are 0.23 and 0.25 Å, respectively. The structural modifications

induced by the enzyme on the TS can be rationalized by considering that they are constituted by two subsystems, the ring ($HOC_6H_4COO^-$) and the bridge (CH_2CO-COO^-), with formal −1 charge and thus a considerable electrostatic repulsion should exist between both fragments. Thus, electrostatic stabilization by a non-homogeneous dielectric environment can diminish the repulsion between both negative charges. As pointed out by Richards and co-workers [25], it is to be expected that charged residues will have an important influence on the substrate. An analysis of the contribution of the amino acid residues of the active site on the quantum region, i.e. $E_{QM/MM}$, reveals that the strongest favorable interactions with R and TS (in both OHin and OHout configurations) are associated with Arg7, Arg90, and Arg116 of the B sidechain and Arg63 and Lys60 of the A sidechain [26]. It is noted that Glu78, that was believed to have an important stabilizing interaction with the substrate, presents a local favorable interaction with the hydroxyl hydrogen atom but a non-favorable one with the total negative charged substrate. Moreover, because of the hydrogen bonds established in the active site, the enzyme favors the intramolecular charge transfer (or electron polarization) from the ring toward the bridge, which is increased from 0.20/0.26 a.u. in the gas phase to 0.38/0.46 a.u. in the enzyme for TS_{OHin}/TS_{OHout}, respectively. This charge transfer process also diminishes the electrostatic repulsion between both subsystems and thus bond breaking (C-O) and bond forming (C-C) distances can be reduced. Thus, our theoretical calculations predict a more polarized but no more dissociative TS in the enzyme than in the gas phase.

In summary, we have for the first time located and characterized two possible TSs for the chorismate conversion to prephenate in water and in BsCM. These TSs have been connected with their respective reactants and products by an IRC procedure in the presence of 488 water molecules and 5573 enzyme atoms, respectively. Although both environments lead to stabilization of one of the TSs (TS_{OHout}), the more specific hydrogen bond interactions present in the enzyme strongly catalyze the reaction. This is effectively more polarized but less dissociative than the corresponding gas phase TS. Electrostatic stabilization and an intramolecular charge transfer process can explain these enzymatically induced changes, while the rate enhancement observed in water comes mainly from a reactant structure destabilization. Our theoretical results provide new information on an important enzymatic transformation and the key factors responsible for efficient selectivity are clarified.

Acknowledgements. This work was supported by DGICYT project PB96-0795.

References

1. Haslam E (1974) The shikimate pathway. Wiley, New York
2. Weiss U, Edwards JM (1980) The biosynthesis of aromatic compounds. Wiley, New York
3. Sogo SG, Widlanski TS, Hoare JH, Grimshaw CE, Berchtold GA, Knowles JR (1984) J Am Chem Soc 106: 2701
4. Copley SD, Knowles JR (1987) J Am Chem Soc 109: 5008
5. Dirggers EM, Cho HS, Liu CW, Katzka CP, Braisted AC, Ulrich HD, Wemmer DE, Schultz PG (1998) J Am Chem Soc 120: 1945
6. (a) Jenks WP (1987) Catalysis in chemistry and enzymology. Dover, New York; (b) Williams IH (1993) Chem Soc Rev 22: 277
7. Gustin DJ, Mattei P, Kast P, Wiest O, Lee L, Cleland WW, Hilvert D (1999) J Am Chem Soc 121: 1756
8. Wiest O, Houk KN (1995) J Am Chem Soc 117: 11628
9. Davidson MM, Gould IR, Hillier IH (1996) J Chem Soc Perkin Trans 2: 525
10. Khanjin NA, Snyder JP, Menger FM (1999) J Am Chem Soc 121: 11831
11. Lyne PD, Mullholland AJ, Richards WG (1995) J Am Chem Soc 117: 11345
12. Carlson HA, Jorgensen WL (1996) J Am Chem Soc 118: 8475
13. Davidson MM, Guest JM, Craw JS, Hillier IH, Vincent MA (1997) J Chem Soc Perkin Trans 2: 1395
14. Warshel A, Levitt M (1976) J Mol Biol 103: 227
15. Dewar MJS, Zoebisch EG, Healy EF, Stewart JJP (1985) J Am Chem Soc 107: 3902
16. (a) Becke AD (1988) Phys Rev A 38: 3098; (b) Becke AD (1993) J Chem Phys 98: 5648; (c) Lee C, Yang W, Parr RG (1988) Phys Rev B 37: 785
17. Frisch MJ, Trucks GW, Schlegel HB, Gill PMW, Johnson BG, Robb MA, Cheeseman JR, Keith T, Petersson GA, Montgomery JA, Raghavachari K, Al-laham MA, Zakrzewski VG, Ortiz JV, Foresman JB, Cioslowski J, Stefanov BB, Nanayakkara A, Challacombe M, Peng CY, Ayala PY, Chen W, Wong MW, Andres JL, Reploge ES, Gomperts R, Martin RL, Fox DJ, Binkley JS, Defrees DJ, Baker J, Stewart JP, Head-Gordon M, Gonzalez C, Pople JA (1995) Gaussian 94, revision D3. Gaussian, Pittsburgh
18. Schlegel HB (1982) J Comput Chem 3: 214
19. Brooks BR, Bruccoleri RE, Olafson BD, States DJ, Swaminathan S, Karplus M (1983) J Comput Chem 4: 187
20. (a) Moliner V, Turner AJ, Williams IH (1997) J Chem Soc Chem Commun 1271; (b) Turner AJ, Moliner V, Williams IH (1999) Phys Chem Chem Phys 1: 1323
21. Chook YM, Ke H, Lipscomb WN, Protein Data Bank ID code 1COM
22. (a) Schmidt MW, Gordon MS, Dupuis M (1985) J Am Chem Soc 107: 1585; (b) Stewart JJP (1993) Quantum Chem Program Exch Bull 13: 42
23. Chook YM, Ke H, Lipscomb WN (1993) Proc Natl Acad Sci USA 90: 8600
24. Andrews PR, Smith GD, Young IG (1973) Biochemistry 12: 3492
25. Lyne PD, Mulholland AJ, Richards WG (1995) J Am Chem Soc 117: 11345
26. This analysis has been carried out by adding amino acid residues to the substrate using the structures optimized in the QM/MM calculations. This method is similar to the ones employed by Bash et al. (Bash PA, Field MJ, Davenport RC, Petsko GA, Ringe D, Karplus M (1991) Biochemistry 30: 5826) and Richards et al. [25]